



3D digital light process bioprinting: Cutting-edge platforms for resolution of organ fabrication

Yun Geun Jeong^a, James J. Yoo^b, Sang Jin Lee^b, Moon Suk Kim^{a,*}

^a Department of Molecular Science and Technology, Ajou University, 206 World Cup-ro, Yeongtong-Gu, Suwon, 16499, South Korea

^b Wake Forest Institute for Regenerative Medicine, Wake Forest School of Medicine, Medical Center Boulevard, Winston-Salem, NC, 27157, USA

ARTICLE INFO

Keywords:

Bioprinting
Digital light process
Resolution
Bioinks
Regenerative medicine

ABSTRACT

Research in the field of regenerative medicine, which replaces or restores the function of human damaged organs is advancing rapidly. These advances are fostering important innovations in the development of artificial organs. In recent years, three-dimensional (3D) bioprinting has emerged as a promising technology for regenerative medicine applications. Among various techniques, digital light process (DLP) 3D bioprinting stands out for its ability to precisely create high-resolution, structurally complex artificial organs. This review explores the types and usage trends of DLP printing equipment, bioinks, and photoinitiators. Building on this foundation, the applications of DLP bioprinting for creating precise microstructures of human organs and for regenerating tissue and organ models in regenerative medicine are examined. Finally, challenges and future perspectives regarding DLP-based bioprinting, particularly for precision printing applications in regenerative medicine, are discussed.

1. Introduction

The field of regenerative medicine is rapidly advancing, driven by the increasing need to replace or restore the function of human organs. These advances are fostering substantial innovations in the development of artificial organs [1,2]. Human organs vary widely in size, from tens of centimeters to micrometers, and comprise complex networks of blood vessels, specialized tissues, and diverse cell types [3,4]. The internal structures of these organs feature microstructures ranging from tens of micrometers to nanometers, necessitating the simultaneous creation of both large-scale and high-resolution tissue structures for effective artificial organ fabrication.

3D printing technology, also known as additive manufacturing or rapid prototyping, emerged in the 1980s as an alternative to traditional manufacturing methods involving molds and machining [5–8]. This technology has evolved into a versatile method for producing customized, complex objects with unprecedented precision. Originally used for creating personalized polymer-based products, 3D printing has expanded its capabilities to create intricately detailed structures with minimal limitations, thereby establishing 3D printing as a key player in various research and industrial sectors.

The fundamental concept of 3D printing involves creating a digital model of the desired object using computer-aided design (CAD) software

[9–11]. This model enables layer-by-layer printing of objects, thereby facilitating high levels of automation, reproducibility, and cost-effectiveness. Such capabilities are particularly valuable for on-demand production of customized items, especially in low-production volume scenarios where digital files can be modified easily. Researchers continuously refine and develop various 3D printing techniques, including inkjet-based, light-based, and extrusion-based methods [12–19].

Among these techniques, light-based polymerization strategies, such as Digital Light Processing (DLP), excel at producing high-resolution printing on a micrometer scale [20–22]. DLP-based 3D bioprinting employs digital light sources, such as ultraviolet (UV), blue light, or near-infrared (NIR) light, to cure photopolymerizable prepolymer solutions layer by layer. This approach enables the construction of complex, high-resolution 3D scaffolds with intricate structural details [23].

DLP printing uses specific light wavelengths to initiate photo-curing or photo-polymerization, creating thermosetting properties that enable the formation of various tissue types (Fig. 1). This process offers superior resolution for the production of intricate structures with high precision. In addition, DLP printing is known for its speed, which allows for faster tissue and organ fabrication than traditional methods such as inkjet-based and extrusion-based methods [24]. A key advantage of this method is the elimination of support materials, which simplifies the

* Corresponding author.

E-mail address: moonskim@ajou.ac.kr (M.S. Kim).

<https://doi.org/10.1016/j.mtbio.2024.101284>

Received 27 July 2024; Received in revised form 27 September 2024; Accepted 1 October 2024

Available online 2 October 2024

2590-0064/© 2024 The Authors. Published by Elsevier Ltd. This is an open access article under the CC BY-NC license (<http://creativecommons.org/licenses/by-nc/4.0/>).

overall process and reduces the need for post-processing steps.

However, despite these advantages, accurately replicating the complex, multiscale architecture of internal organs remains a significant challenge in DLP-based organ printing. Internal organs consist of intricate structures that range in size from large centimeter-sized features to microscopic components that span only a few micrometers [25]. The ability to precisely replicate multiscale features in a single printed construct is a formidable challenge. In addition to structural complexity, ensuring the functionality and biological compatibility of printed tissues further complicates the process.

The success of these techniques depends heavily on various factors, including the printer characteristics and the specific fabrication parameters employed during printing. These factors influence critical aspects of the final product, such as organ resolution, production time, and overall quality and functionality of the tissue construct. Furthermore, organs of different sizes and complexity require distinct considerations for model design and topological optimization. Balancing resolution and production speed while ensuring organ structural and functional integrity remains a key challenge.

This review presents an overview of the fundamental principles of DLP bioprinting, traces the evolution of light-based printing technology, and discusses the current state of DLP printing techniques. Next, cutting-edge bioinks currently used for organ tissue construction are examined. These bioinks play crucial roles in the biocompatibility, mechanical properties, and long-term viability of printed tissues. Finally, this review discusses the advantages and limitations of DLP bioprinting for fabricating diverse organs and provides insights into its potential applications and challenges to be addressed for clinical progress.

2. DLP printing

2.1. DLP printer

DLP was originally developed and patented by Larry Hornbeck at Texas Instruments in 1987 [26].

This technology is based on optical micro-electro-mechanical systems and employs a digital micromirror device (DMD), which comprises an array of microscopic mirrors arranged in a matrix on a semiconductor chip. In DLP projectors, these micromirrors reflect light to create images, and they are synchronized with the DLP printer's software to form printing patterns. Each micromirror corresponds to one or more pixels in the projected image, with a pixel pitch as small as 5.4 μm , enabling the production of highly detailed and high-resolution prints.

The DMD consists of millions of tiny mirrors that rapidly toggle on and off according to the 2D digital patterns uploaded into the DLP program software. The synchronized movement of these micromirrors determines the grayscale levels by adjusting the ratio of on-time to off-time. Each mirror tilts between two positions to either reflect light through a lens or direct it away to a heat sink, known as a light dump, depending on the printing or projection requirements. This dynamic movement controls the rendering of the image on the print or projection surface.

The resolution in DLP systems is defined as the number of pixels displayed on the screen or in the printed output. Common DMD matrix sizes include 800 \times 600, 1024 \times 768, 1280 \times 720, and 1920 \times 1080, with the number of mirrors directly affecting the system resolution. However, due to a process called wobulation, the effective resolution can sometimes be halved as the mirrors oscillate to enhance image sharpness and detail. DLP technology is versatile and can function independently of the light source, allowing it to be used in various types of illumination. Historically, high-pressure xenon arc lamps have been the primary light source in DLP systems. However, modern pico (ultra-

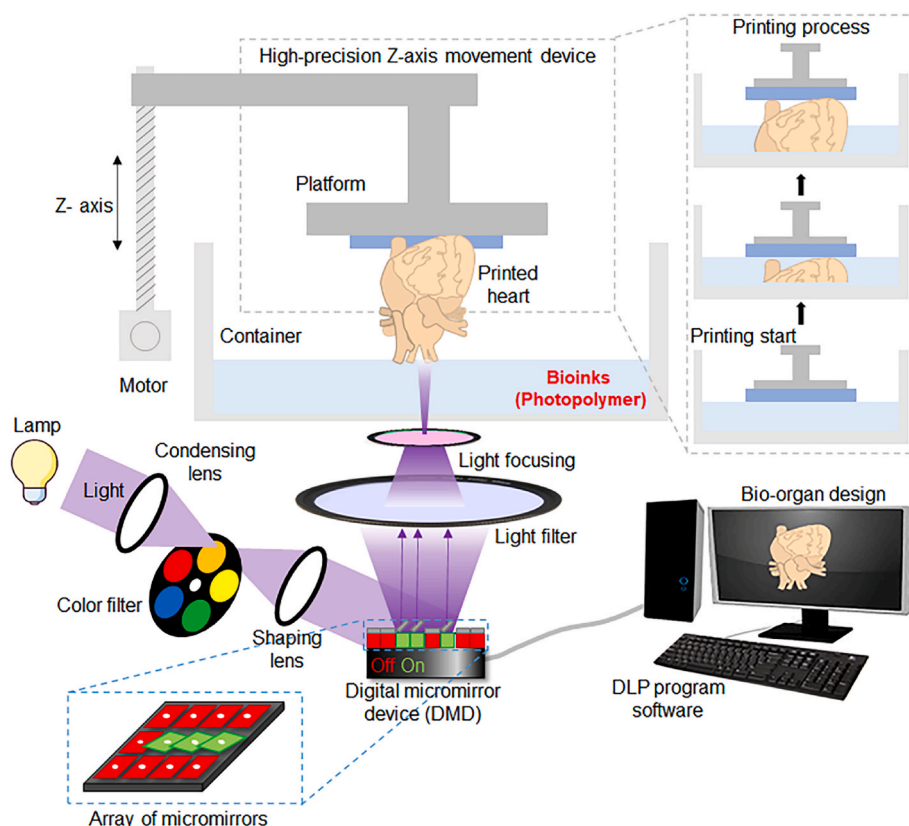


Fig. 1. Schematic diagram of the target organ bioprinting process using DLP-based 3D printing technology.

small) DLP projectors often use high-power LEDs or lasers for illumination, offering greater energy efficiency and compactness [27]. This versatility makes DLP an adaptable and widely used technology in various applications, including projection systems and advanced 3D printing solutions.

Compared to standard extrusion-based printers, DLP printers excel at rapidly producing fine microstructures by projecting digital patterns onto the bioink. Their ability to create high-resolution structures at high speeds makes DLP printing particularly well-suited for a range of bio-printing applications. The fundamental components of a DLP printer include the following key elements.

- Digital projection device: Digital patterns are projected onto the photopolymerizable liquid bioink.
- Light source system: This system provides the necessary light to cure the bioink.
- Container with liquid bioink: The bioink is housed in this container during the printing process.
- High-precision Z-axis movement device: This device allows precise vertical movement for creating detailed layers.
- Control program: Manages printer operation and movement.
- Auxiliary equipment: Supports core components and enhances functionality.

Technological advancements have led to the development of diverse DLP printers tailored to specific printing requirements (Table 1) [28]. The resolution in DLP platforms, which rely on DMDs, is fundamentally constrained by the width of light reflected from each individual micromirror [29]. To achieve higher resolution, it is crucial to precisely control both the exposure time and the positions of the print head during operation. In addition to these factors, adjusting the viscosity of the bioink by increasing its density and reducing light penetration can further enhance the printing resolution. This strategy helps to refine the accuracy of the printed structures.

Most commercialized DLP printers now operate at light wavelengths ranging from 365 to 405 nm, allowing them to achieve impressive print resolutions between 15 and 50 μm [30]. These technological advancements have significantly expanded the potential applications of DLP printing, particularly in high-impact fields such as tissue engineering, organ fabrication, and medical research. As DLP printing technology continues to evolve, its growing precision and versatility make it an increasingly valuable tool for developing complex biological constructs and advancing biomedical research.

2.2. Selection criteria of bioink for DLP printing

The selection of bioinks for DLP printing in organ fabrication is governed by several critical factors.

1. Number of reactive functional groups: The quantity of reactive groups influences the reactivity and mechanical properties of the bioink.
2. Ink viscosity: Optimal viscosity ensures printability and high-resolution of the final structure.
3. Reaction kinetics: The speed and accuracy of the printing process are influenced by reaction kinetics.
4. Hydrophobicity/hydrophilicity: This property influences the interaction of the bioink with the cellular environment.
5. Shrinkage: Dimensional stability of the printed structure is influenced by shrinkage.
6. Cost: Economic viability is essential for large-scale applications.
7. Shelf life: Practicality of the bioink is determined by its shelf life.
8. Volatility: Safe handling and storage are influenced by bioink volatility.
9. Mechanical and functional properties: The bioink must meet the desired performance characteristics of the printed organ.

Table 1

Overview of various performance metrics for commercially available DLP printers [28].

Manufacturer	Product name	Pixel size (μm)	Wavelength (nm)	Build size (mm^3)	Layer thickness (μm)
BMF	S230	2	405	50 \times 50 \times 50	5
Acra3D	Pico 2HD 27	6.7	385; 385; 405	19.4 \times 12.1 \times 70	25
Kudo3D	Micro	15	365; 385; 405	15 \times 15 \times 150	5
B9creations	B9 Core 530	15	405	58 \times 32 \times 127	20
EnvisionTec	Perfactory 3	23	385	90 \times 67 \times 180	25
RapidShape	D90 4K	23	385	232 \times 137 \times 150	30
MakeX	One Pro25	25	405	310 \times 310 \times 450	5
Asiga	Pico 2HD 27	27	385; 405	53.4 \times 30.5 \times 70	1
MiiCraft	Profession 120	30	385; 405	120 \times 67 \times 190	12.5
Cadworks3D	M50	30	365; 385; 405	57 \times 32 \times 120	5
Rapid Shape	S30+	34	405	133 \times 75 \times 155	50
Genera	G2	50	385	192 \times 108 \times 370	20
XYZprinting	Nobel Superfine	50	405	64 \times 40 \times 120	25
Flashforge	Hunter	50	N	120 \times 68 \times 150	25
Autodesk	Ember	50	405	64 \times 40 \times 134	50
Carima	IM	75	405	192 \times 108 \times 200	20
Anycubic	Photon Ultra	80	405	102 \times 57 \times 165	10
Cellink's	BIONOVA X	10	405	19.2 \times 10.8 \times 9	10
	LUMEN X	35	405	68 \times 38 \times 100	35
Readily 3D	Tomolite	14	405	12.5 \times 12.5 \times 20	50

10. Toxicity: Nontoxicity of both the printed 3D structure and residual bioink is paramount to ensure biocompatibility.

These criteria ensure that the bioink is suitable for the specific type, strength, and size of the bio-organ to be printed.

The reactivity of the ink composition is significantly influenced by the number of reactive functional groups. A high concentration of reactive groups can accelerate the reaction rate at the onset of light irradiation, leading to rapid viscosity increases and the formation of

denser and more solid three-dimensional networks. Although beneficial for fabricating hard tissues, such rapid viscosity increases can also result in a significant proportion of unreacted functional groups within the polymer, potentially causing issues.

In polymer chemistry, free-radical polymerization is a method in which polymers are formed through the continuous addition of free-radical building blocks, also known as repeat units [31]. In the context of DLP printing, free radicals are typically generated from initiator molecules via various mechanisms. The polymerization process begins with the initiation step, at which an active center is created that allows the growth of the polymer chain. However, not all monomers react uniformly to a given type of initiator, and the choice of initiator is crucial for the success of the process.

The polymerization process begins with the initiation step, at which an active center is formed, allowing the growth of the polymer chain. However, not all monomers are reactive to each type of initiator. DLP printing inks are primarily composed of free-radical polymerizable components formulated with highly reactive acrylate and methacrylate functional groups [32]. These groups initiate polymerization through well-established mechanisms when exposed to light. In the propagation step, photogenerated radicals react with acrylate or methacrylate monomers, increasing their molecular weight as the polymer chain extends. This chain growth continues until the termination step, which halts the reaction and completes the polymerization process. Acrylate-based inks, which are known for their rapid printing speed, high resolution, and nozzle-free printing, have become the industry standard for DLP printing.

During the chain propagation step, photogenerated radicals react with acrylate or methacrylate monomers, resulting in an increase in

molecular weight as the polymer chain extends. This process continues until the termination step, at which the reaction stops, thereby completing the polymerization. Acrylate-based inks have become the industry standard due to their high printing speed, high resolution, and nozzle-free printing.

Fig. 2 illustrates common monomers and oligomers with an acrylic backbone. Radical initiation is most efficient for the carbon-carbon double bonds of vinyl monomers and the carbon-oxygen double bonds of aldehydes and ketones. Upon light exposure, the acrylate groups in bioink trigger polymerization, leading to the formation of highly reactive polymers or cross-linked structures. This pathway, which is fundamental to the photopolymerization process in DLP printing, has been extensively studied.

However, leftover acrylate-reactive groups in 3D-printed structures can pose a cytotoxicity risk, primarily due to the leaching of unreacted groups from the printed material. Research has indicated that these residual acrylate groups may induce mucosal irritation and tissue sensitization [33,34]. To mitigate potential biotoxicity, unreacted acrylate groups can be effectively removed by washing and post-processing the printed structures, steps that are essential for reducing potential biotoxicity in medical applications.

To address the toxicity issues associated with acrylate groups, alternative bioinks incorporating different photoresponsive functional groups, such as vinyl, vinyl ether, thiol-ene, and epoxy-based systems, are actively being explored. Moreover, thiol-ene/phosphorus systems, epoxies, and polyethylene glycol diacrylate (PEGDA) are integrated into interpenetrating network (IPN) hydrogel matrices, improving the mechanical and physiological properties of 3D-printed structures [35,36]. These additives reduce polymer shrinkage, alleviate internal stress, and

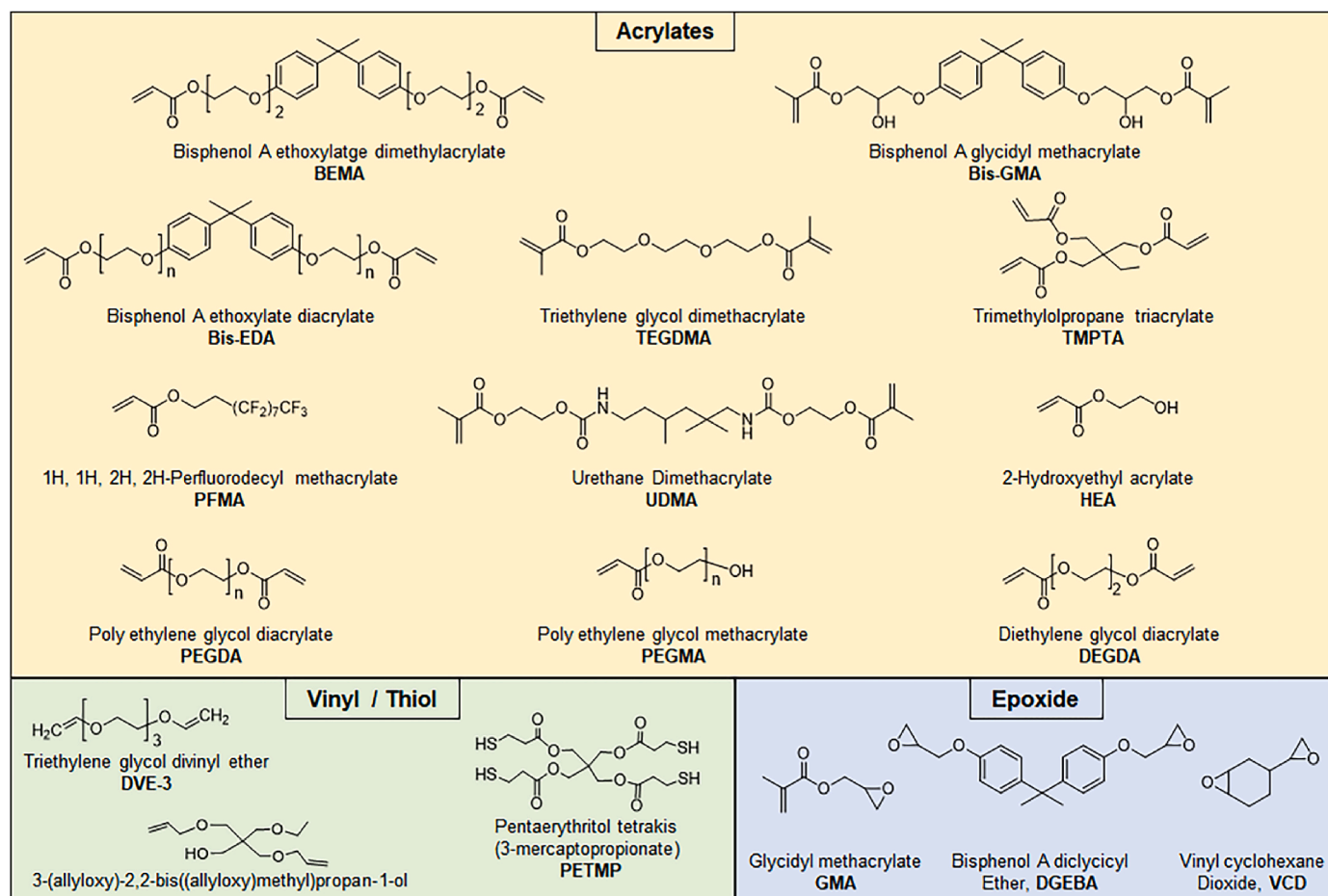


Fig. 2. Chemical structures of commercially available monomers and oligomers with acrylic backbones for use in DLP 3D printing applications.

modulate conversion rates during the printing process.

Despite these advancements, the mechanical and elastic properties of 3D-printed structures, particularly those designed for artificial organs, are heavily influenced by the degree of crosslinking in the primary polymer used in bioinks [37–45]. The design of the main polymer is critical because it determines the mechanical properties and stress distribution of the final structure [46]. Low-molecular-weight reactive species, due to their low viscosity, enhance mobility within the printed structure, reducing post-reaction shrinkage through a temporary dilution effect. In these systems, the propagation phase follows diffusion-controlled dynamics, where the limited mobility of the macro-radical chain ends leads to the formation of heterogeneous networks with varying crosslinking densities. This heterogeneity plays a significant role in determining the overall performance and suitability of 3D-printed structures for various applications, such as regenerative medicine and drug delivery.

An important consideration when selecting bioinks for DLP printing, especially when targeting bioprinted cells, is the refractive index mismatch between the bioink and the cells or cytoplasm. The light scattering effect caused by the presence of a high density of cells can reduce printing resolution and lower pattern accuracy, which ultimately affects the quality and precision of printed constructs.

In summary, the selection and design of bioinks for DLP printing requires careful consideration of various factors to achieve the desired mechanical, physiological, and functional properties while ensuring the biocompatibility and safety of the final printed structures.

2.3. Types of bioinks used in DLP printing

Natural biomaterials from plants and animals exhibit unique and complex components, microstructures, and physiological properties. These materials offer exceptional biological support for cell attachment and growth through diverse functional sets, making them ideal for artificial organ design.

Recent advancements have led to the development and application of various natural and synthetic polymer-based bioinks for DLP 3D printing, including extracellular matrix (ECM), collagen, gelatin, hyaluronic acid (HA), polyvinyl alcohol, and PEG. However, natural biomaterials have limited availability of photopolymerizable functional groups.

ECM materials naturally occurring in the body form networks that combine softness, rigidity, and elasticity to provide mechanical support and structural integrity to human tissues and organs. Recent advancements have led to the development of several methacrylated ECM-based materials as DLP 3D printing inks, demonstrating significant potential in this field [47–50].

Collagen, the most abundant protein in mammals, is a major structural protein in the ECM in various connective tissues [51]. Renowned for its biocompatibility and multiple bioactivities, collagen is a widely explored bioink. Most collagen hydrogels originate from type I collagen, which constitutes approximately 90 % of the protein mass. As a member of the fibrillar-forming collagen family, type I collagen comprises three alpha helices that form a triple-helix structure. Under physiological conditions (neutral pH and 37 °C), collagen molecules self-assemble into fibrils, forming a hydrogel [52]. This self-assembly property renders collagen a potential bioink for extrusion-based printing. However, due to its inherent low viscosity, most extrusion-based printing studies have required increased collagen concentration or the addition of thickeners to achieve stable extrusion.

Concurrent research has explored the use of methacrylated collagen (Col-MA)-based bioinks in DLP printers. Although Col-MA demonstrated suitable printability, the inherent self-assembly dynamics of collagen molecules significantly influence the printing. Therefore, controlling mechanical properties and preventing structural collapse remain challenges when using Col-MA bioinks in DLP printing. To address these limitations, innovative DLP printing methods are required to accelerate

and control gelatinization, enhance bioink stability, and increase the crosslinking density of printed artificial organs [53].

Gelatin, a natural biopolymer derived from animal collagen, is produced through the irreversible denaturation of animal collagen found in the skin, cartilage, and tendons. Gelatin shares structural similarities with collagen but exhibits distinct thermal properties. It is highly sensitive to temperature, dissolves in water above 40 °C, and forms a gel below this temperature. Despite its favorable biological properties, including an inherent Arg-Gly-Asp (RGD) motif, low immunogenicity, biocompatibility, and biodegradability, gelatin's inherent inadequate mechanical properties limit its use as an ink for DLP printing. To enhance the printability of gelatin for DLP applications, methacrylated gelatin (Gel-MA) was developed [54–58]. By incorporating methacrylated groups, Gel-MA becomes photoreactive, enabling crosslinking through exposure to UV light in the presence of a photoinitiator. This modification significantly expanded the use of gelatin as a bioink for DLP printing.

Hyaluronic Acid (HA), a polysaccharide, is particularly noteworthy as a biomaterial for wound healing, angiogenesis, tendon regeneration, and cartilage regeneration because of its low immunogenicity. Methacrylated HA (HA-MA), which is used as a bioink, exhibits excellent biocompatibility and is particularly advantageous for the DLP printing of biological organs [59–61]. However, the rapid degradation of HA-based 3D structures within approximately one week necessitates the incorporation of HA-MA along with other materials to maintain stable mechanical properties in vivo.

Following the development of Col-MA, Gel-MA, and HA-MA, researchers have developed methacrylated derivatives of other natural biomaterials such as pectin and silk. Despite their potential in designing artificial organs, natural biomaterials face significant challenges such as batch-to-batch variability, rapid degradation, poor mechanical properties, and limited processability, hindering their clinical translation.

PEG is highly valued in biomedical applications because of its hydrophilic nature, water solubility, and biocompatibility [62]. In aqueous solutions, PEG is neutral, exhibits high mobility, and retains hydration, making it an excellent candidate for biomaterial development. PEG-based polymers, particularly those with reactive (meth)acrylate functional groups, such as PEGDA, have gained popularity for photopolymerization in DLP printing [63]. PEGDA-based bioinks offer a versatile platform for fabricating soft scaffolds with customizable physical, chemical, and mechanical properties, making them highly applicable to tissue engineering [64–67]. These scaffolds exhibit a high swelling ratio due to their porous structure, which significantly increases the surface area exposed to biological media, thereby enhancing absorption.

Understanding and monitoring the volumetric changes caused by swelling and water uptake are crucial for maintaining print resolution and structural fidelity. The swelling kinetics of 3D-printed PEGDA scaffolds, especially under physiological conditions in cell culture media, are essential for optimizing their performance in biomedical applications [68]. Therefore, studying the behavior of scaffolds when exposed to various biological environments is crucial.

Poly(glycerol-co-sebacate) (PGS), a biodegradable elastomer first developed in 2002 by Robert Langer's group, has demonstrated particular utility in dynamic tissue environments [69]. PGS is a copolymer of glycerol and sebacic acid, both naturally occurring components used in FDA-approved medical devices. In a significant advancement, Singh et al. introduced PGS-methacrylate (PGSM), a modified version of PGS that can be rapidly photo-crosslinked via DLP printing [70]. PGSM was used to create 3D-printed cylindrical conduits with an average modulus of 3.2 MPa, which closely matches the stiffness range of native nerve tissue (0.45–3.0 MPa). In vivo studies showed that PGSM-based nerve guidance conduits successfully supported axonal regeneration across the scaffold and into the distal stump within 21 days, making it a promising material for nerve tissue engineering.

In DLP printing, optimizing the exposure time and post-processing steps is essential for improving the mechanical properties of printed

bioink structures [71]. Extended exposure times increase the cross-linking density, which strengthens or rigidifies the scaffold. However, careful control is required to avoid over-curing, which may compromise the scaffold's flexibility. Post-processing techniques such as thorough washing to remove any uncured bioink and additional curing under controlled conditions, reinforce the printed network and improve its durability. Methods such as thermal annealing can also relieve internal stresses in the material, further enhancing the scaffold robustness and reliability.

Despite these significant advancements, considerable knowledge gaps remain in the molecular design of bioinks for DLP 3D printing. Key factors such as dimensional stability, physical isotropy and mechanical behavior, and viscoelastic properties require further exploration to optimize bioink formulations. Moreover, the influence of printing direction and light orientation on the physical anisotropy of printed structures remains a crucial area for further research. To fully realize the potential of DLP 3D printing in organ fabrication, it will be essential to develop bioinks that maintain consistent physical, chemical, and mechanical stability while preserving structural integrity, paving the way for future innovations in the field.

2.4. Photoinitiators

DLP printing relies on photoinitiators with high absorption coefficients to efficiently convert light energy into reactive species, such as radicals or cations, which initiate the polymerization process in bioinks [72–74]. These photoinitiators are crucial because they absorb light emitted by the DLP projector, driving the chemical reactions necessary

to solidify liquid bioinks into precise 3D structures. A key aspect of photoinitiators is their sensitivity to specific light wavelengths, which must match the DLP light source to ensure effective curing. This alignment directly influences the polymerization speed, print accuracy, and mechanical properties, ultimately affecting the overall print quality. Furthermore, photoinitiators must be compatible with various bioink formulations and exhibit minimal post-cure shrinkage to maintain the precision and stability of the printed scaffolds.

Photoinitiators with high molar absorption coefficients over a broad spectral range (200–700 nm) are currently widely used (Fig. 3). Upon exposure to UV light, these photoinitiators trigger a chain reaction with monomers or oligomers such as activated acrylates, leading to the rapid formation of 3D structures. Although UV-based photoinitiators are effective, they have certain limitations. The shallow penetration depth of UV light necessitates thin printing layers, ranging from a few micrometers to less than 100 μm , which can limit the scale of objects that can be printed. In addition, prolonged UV exposure can degrade bioink components and cause cellular damage in prints containing viable cells, potentially leading to chromosomal and genetic instability. These issues can hinder the printing process, especially for large structures such as artificial organs.

To address these challenges, near-infrared (NIR) photoinitiators have been developed, offering several advantages due to their activation at longer wavelengths. NIR photoinitiators operate under milder conditions, significantly reducing the risk of cellular damage. They also allow deeper light penetration, facilitating the printing of larger and more complex structures. Furthermore, NIR photoinitiators are more compatible with various cell types, thereby improving the viability of

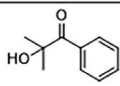
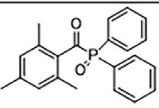
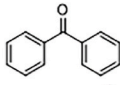
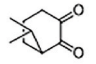
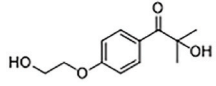
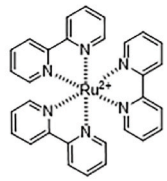
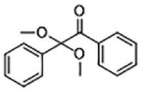
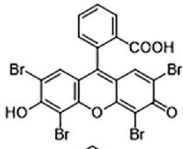
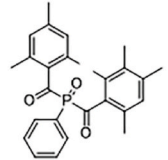
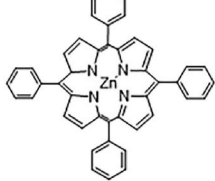
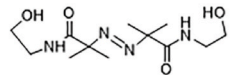
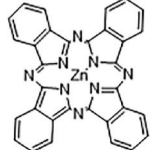
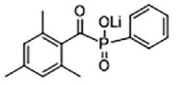
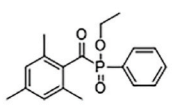
Name	Chemical Structure	Maximum absorption	Name	Chemical Structure	Maximum absorption
2-Hydroxy-2-methyl-1-phenylpropan-1-one (Irgacure 1173)		245 nm	Di phenyl (2,4,6-trimethylbenzoyl) phosphine oxide (Darocure TPO; Lucirin TPO)		380 nm
Benzophenone		253 nm	Camphorquinone (CQ)		468 nm
2-Hydroxy-4'-(2-hydroxyethoxy)-2-methylpropiophenone (Irgacure 2959)		279 nm	Tris(2,2'-bipyridyl) dichlororuthenium(II) / Ru(bpy) ₃ Cl ₂		453 nm
2,2-Dinethoxy-2-phenylacetophenone (Irgacure 651 or DMPA)		340 nm	Eosin Y		524 nm
Phenyl bis(2,4,6-trimethylbenzoyl) phosphine oxide (BAPO, Irgacure 819)		370 nm	Zinc tetraphenylporphyrin (ZnTPP)		530nm
2,2'-Azobis [2-methyl-n-(2-hydroxyethyl) propionamide] (VA-086)		375 nm	Zinc phthalocyanine (ZnPC)		686 nm
Lithium phenyl (2,4,6-trimethylbenzoyl) phosphinate (LAP)		375 nm			
Ethyl (2,4,6-trimethylbenzoyl) phenylphosphinate (Lucirin TPO - L)		379 nm			

Fig. 3. Chemical names, structures, and maximum absorption wavelengths of photoinitiators used in 3D photopolymerization.

bioprinted tissues and organs.

Recent advancements in DLP photoinitiators have expanded the available options, offering varying resolutions that are suitable for various printing applications (Table 2) [75–99]. The selection of the photoinitiator is critical for determining the resolution and quality of the printed structures. However, despite progress in the development of NIR photoinitiators, several challenges remain, including their compatibility with bioink materials, potential toxicity, and environmental sustainability. Addressing these challenges is essential for optimizing photoinitiator performance and advancing 3D bioprinting technology.

3. Resolution in organ DLP bioprinting

Recent advances in optical design have significantly enhanced DLP capabilities, enabling the fabrication of implantable microtissue models for diverse biomedical and regenerative medicine applications. Fig. 4 illustrates the variability in the size of different organs. For artificial organ transplantation, precise replication of organ-specific dimensions is imperative, which requires the incorporation of cells and biologically active factors into printed structures.

A fundamental trade-off exists between the print area and the print resolution in DLP bioprinting. The print resolution, which is defined as the smallest feature size that can be accurately produced, is a critical factor in replicating the intricate details of natural tissues. Although higher resolution enables precise replication of complex tissue structures, it typically requires a reduction in the overall print area.

Table 2

Bioprinting performance by photoinitiator type for DLP bioprinting (chemical structures of photoinitiators are shown in Fig. 3).

Photoinitiator	Light λ (nm)	Bioinks	Resolution (μm)	Cell-viability	Ref.
LAP	365	PEGDA, GelMA	~20	Medium	75–77
LAP	365	GelMA-PEGDA, GelMA-HA, GelMA-GMHA	50	Medium	78–82
LAP	380	GelMA-PEGDA	15–50	Low	83
LAP	395	HAMA, GelMA	50	High	84,85
LAP	405	PEGDA-GelMA, PEGDA	10–50	High	86,87
LAP	405	CHI-MA	20–50	High	88
LAP	405	CMC-MA	20–50	High	89
LAP	405	SF-GMA	10–50	High	90
LAP	405	PEGDA	10–50	High	91
Eosin Y	400–700	GelMA, PEGDA	50	High	92,93
Eosin Y	405	SF-PEG4A (2 % w/v)	20–50	High	94
Irgacure 819	380	BPADA-GMA-BA	20–50	NA ^b	95
Ru:SPS	400–700	PVA-MA, PEGDA	20–50	High	96,97
UCNP@LAP	980	GelMA	>100	High	98
DCPI	375 & 520	PETA	<10	NA	99

[Ru:SPS]: Tris(2,2'-bipyridyl)dichlororuthenium(II) sodium persulfate, [UCNP]: Upconversion nanoparticle, [DCPI]: dark-curing photoinitiator [Diphenyl(2,4,6-trimethylbenzoyl)phosphine oxide].

GelMA: Gelatin methacrylate, PEGDA: Polyethylene glycol diacrylate, HAMA: Hyaluronic acid methacrylate, CHI-MA: Chitosan methacrylate, CMC-MA: Carboxymethyl cellulose methacrylate, SF-GMA: Silk fibroin glycidyl methacrylate, BPADA: Bisphenol A ethoxylate diacrylate, PVA-MA: Polyvinyl alcohol methacrylate, PETA: Pentaerythritol tetraacrylate, UCNP@LAP: LAP coated on an up-conversion nano particle, SF-PEG4A: Silk fibroin incorporated 4-arm polyethylene glycol acrylate.

Current DLP technology typically achieves resolutions in the tens of micrometers range. This limitation is primarily attributed to the photochemistry involved in the crosslinking process, which constrains the lateral resolution beyond the minimum laser spot or pixel size. In addition, the layer thickness is linked to the light penetration depth, which affects the vertical resolution.

Despite optimizations for micrometer-resolution DLP printing, practical limitations remain. Optimal feature dimensions often converge around 100 μm laterally and 300 μm vertically, with layer spacings between 40 and 50 μm in hydrogel-based systems [100,101]. However, recent technological advancements have demonstrated the potential for higher resolution. Bhusal et al. achieved line thicknesses as low as 15 μm using acellular PEGDA, which approaches the size of individual cells, demonstrating the potential of the technology for high-resolution bioprinting [102].

You et al. included iodate in the bioink to increase the light scattering by 10-fold to alleviate the decrease in bioprinting resolution due to the increased cell density in the bioink [103]. For the bioink with a density of 0.1 billion cells per milliliter, a fabrication resolution of 50 μm was achieved. This technology has confirmed the possibility of 3D bioprinting with high cell density, high viability, and high resolution simultaneously. This work serves as a great demonstration of utilizing DLP printing technology to tackle large-scale organ biofabrication without sacrificing printing resolution due to the light scattering effect. Nevertheless, the cell density in this study was still lower than the physiologically observed level (1 billion to 3 billion cells/ml), and this issue requires continuous improvement for clinical application.

Typically, DLP resolution represents a compromise between the desired feature size and sample size, which is influenced by the projector resolution and optical configuration [104–106]. To circumvent these limitations, an innovative approach combining a dual-color photoinitiator system with light-sheet excitation and DLP was developed. This method reduces layer thickness and eliminates the need for layer-by-layer deposition, achieving horizontal and vertical resolutions of 25 μm and 50 μm , respectively, in acellular resin.

DLP-based 3D printing encompasses Projection Micro Stereolithography (P μ SL) [107]. P μ SL excels at printing complex 3D structures with exceptional resolutions ranging from 0.6 to 30 μm , while maintaining relatively large print areas of up to approximately 90 mm \times 50 mm. This technique exemplifies DLP's potential for high-resolution and large-print areas.

Nevertheless, continuous advancements in ink formulations, photoinitiator design, and printer systems are essential for enhancing printing resolution.

4. The advancements of DLP-based 3D organ printing

3D bioprinting offers a novel approach to tissue engineering by enabling the precise distribution of cells, materials, and biological elements within structures. DLP-based 3D bioprinting excels at producing tissue constructs under mild conditions, minimizing damage to sensitive biological constituents. This technology has been used to fabricate various tissues and organ models, including liver, heart, blood vessels, and cancer models (Table 3) [108–119]. This section describes the results of DLP-based artificial organ fabrication.

3D DLP bioprinting offers several key advantages over traditional inkjet and extrusion-based methods when it comes to fabricating intricate tissue constructs [120,121]. This technique is notably faster, more precise, and gentler. Its printing speed is approximately 1000 times faster than conventional nozzle-based approaches such as inkjet or extrusion bioprinting. Moreover, DLP technology achieves an impressive lateral resolution of 6 μm on both the X and Y axes, ensuring high accuracy in the printed structures. Unlike inkjet and extrusion bioprinting, which can expose cells to damaging shear stresses during the printing process, DLP printing operates in a way that avoids such stress, preserving cell viability and function. This characteristic makes DLP

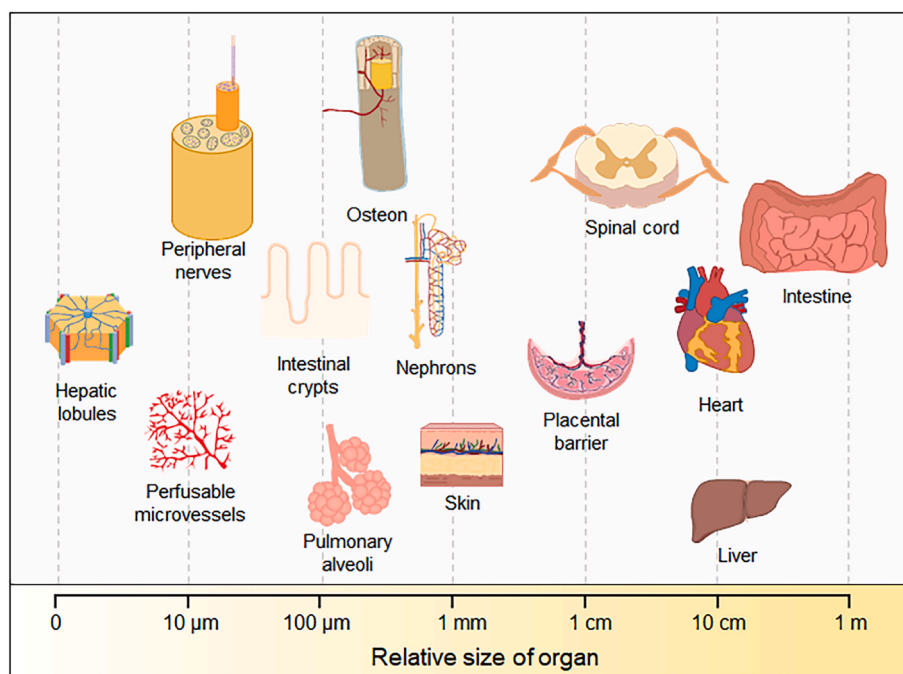


Fig. 4. Relative sizes of the organs represented on a logarithmic scale.

bioprinting especially suitable for creating complex and delicate living tissues, including those requiring intricate vascular networks, such as organs like the liver and lungs.

The liver is the largest internal organ and gland in the human body. Using a DLP-based 3D printer, Ma et al. encapsulated three types of cells—human induced pluripotent stem cell (hiPSC)-derived hematopoietic progenitor cells (HPC), human umbilical vein endothelial cells (HUVEC), and adipose-derived stem cells—to print numerous micro-hexagonal structures [122–126]. By analyzing cell morphology, liver-specific gene expression levels, metabolic products, and cytochrome P450 induction, the authors determined that hiPSC-HPCs in the printed liver model closely resembled human liver cells. The results indicate that the microstructure and supporting cells promote the maturation and maintenance of hiPSC-HPC functions.

A simplified model incorporating HUVEC and HepG2 cells was developed [127]. Grigoryan et al. also fabricated an artificial liver with functional vascular topology using DLP 3D printing [87]. This vascularized liver with liver cell aggregates exhibited 60-fold higher albumin promoter activity than tissues containing single liver cells. Furthermore, DLP 3D-printed vascularized liver tissue exhibited enhanced integration with the host after *in vivo* transplantation.

Bones are dynamic organ tissues with inherent regeneration capacity. However, severe bone defects generally require bone replacement or surgical intervention. DLP 3D bioprinting offers a precise solution for the fabrication of bone scaffolds by arranging various cells within the scaffold to form bioengineered bone structures [128]. DLP 3D printing enables the creation of bone tissue engineering scaffolds that perfectly fit bone defect sites and the accurate printing of internal bone structures, facilitating the smooth supply of bio-nutrients and growth factors within artificial bone scaffolds [129].

DLP-printed scaffolds exhibit exceptional accuracy for promoting cell adhesion, proliferation, and maturation of damaged bone microstructures. Recent studies have explored the use of methacrylate polyvinyl alcohol (PVA-MA) and Gel-MA loaded with mesenchymal stem cells (MSCs) as a DLP bioink to produce bone and cartilage tissue [130]. Jiang et al. manufactured a platelet-rich plasma-loaded Gel-MA (PRP-Gel-MA) ink using the DLP printing technique and implanted it in an injured rabbit for osteochondral defect repair [131]. These

scaffolds exhibited successful cartilage regeneration and integration with native tissue after 18 weeks.

DLP 3D printing has been used to fabricate a scaffold for regenerating the spinal cord, a complex and precise cylindrical structure composed of nerve fibers and associated tissues. Yuan et al. fabricated a 3D biomimetic hydrogel scaffold tailored to the size of a rodent spinal cord within seconds [132]. The printed scaffold facilitated regeneration of axons in the neural progenitor cells (NPCs) housed within it, resulting in regeneration of damaged axons and synapses with NPCs, thereby enhancing recovery of spinal cord function.

Andres J. Garcia's group has made significant strides in the fabrication of permeable hydrogels, which are essential for replicating the microphysiological environment *in vitro* [133]. They developed a cost-effective, versatile, and ultrafast methodology for creating complex-shaped permeable microchannels within photopolymerizable hydrogels without requiring specialized equipment or complicated protocols. The team photopatterned PEG-norbornene hydrogels using a one-step UV photo-triggered crosslinking process with a photomask printed on Mylar transparency film. This innovative approach enabled the precise printing of permeable microchannels, broadening the potential applications of these hydrogels in biomedical research. In a dynamic culture setup with continuous fluid perfusion through the microchannels, human endothelial cells successfully formed functional, confluent endothelial monolayers. These monolayers remained viable for at least 7 days and exhibited responsive behavior to inflammatory stimuli, indicating their potential for vascular biology studies.

In a separate advancement, David Juncker's group has made significant contributions by creating 3D-printed structures with varying porosity and oxygen permeability, achieving thicknesses as thin as 27 μm . They used nanoporous PEGDA inks to address the challenges of fabricating intricate geometries, including organ-on-a-chip models [134]. A notable highlight of their research was an organ-on-a-chip model that featured a gyroid scaffold with a central opening filled with dark spheroids. This model exhibited excellent gas permeability, biocompatibility, and cell adhesion, demonstrating the potential of developing functional tissue models that closely mimic *in vivo* environments.

Similarly, Yaling Liu's group developed an innovative maskless

Table 3
Resolution of DLP-bioprinted organs using various bioinks and cell types.

Bioprinted organ	Bioink/Cell composition	PI	λ (nm)	Resolution (μm)	Ref.
Liver	GelMA, HAGM, pluripotent stem cells-derived hepatic progenitor cells and HUVECs	LAP	365	25	108
Liver	GelMA, dECM and human-induced hepatocytes cells	LAP	365	–	109
Cardiac muscle	GelMA, mouse ventricular cardiomyocytes. Support and cantilever:HAGM, PEGDA	LAP	365	1	110
Cardiac muscle	PEGDA, BPADA, Human-induced pluripotent stem cell	Irgacure-819	405	25	111
Vascular	HUVEC-laden PEGDA and C3H10T1/2 fibroblast-laden collagen	LAP	380–700	100	112
Vascular	GelMA and PEGDA	LAP	380	15	113
Bone	GelMA, C2C12, HUVEC, fibroblast, hMSCs, osteoblast	LAP	385	25	114
Lung	GelMA, PEGDA, HUVEC, Human lung epithelial cells, fibroblast	LAP	405	50	115
Ear	GelMA, CAM (Cartilage acellular matrix), Microtia chondrocytes	LAP	405	–	116
Cartilage	SF-GMA, NIH/3T3 mouse fibroblast cell	LAP	365	30	117
Ocular	GelMA, Conjunctival stem cells	LAP	365	70	118
Brain tumor	GelMA, GMHA, glioma stem cells, astrocytes, neural precursor cells, macrophages	LAP	–	–	120

lithography-based rapid prototyping method for fabricating microfluidic devices in situ. This approach, known as image-guided in situ maskless lithography (IGIs-ML), combines image-assisted photopolymerization with advanced flow control techniques [135]. As a single-step UV polymerization process, IGIs-ML can be seamlessly integrated into existing in situ polymerization platforms, streamlining the fabrication process. Furthermore, the authors demonstrated the potential for incorporating this method into SLA or VAT polymerization processes provided that suitable imaging and pre-polymer flow control strategies are implemented. This integration could significantly enhance the efficiency and versatility of microfluidic device production, paving the way for more complex applications in biomedical engineering.

5. Challenges and future perspectives in DLP-based bioink 3D printing

DLP-based 3D printing has become a leading method for producing intricate, highly customized products with exceptional precision and speed. This method significantly reduces processing demands while enabling the creation of complex structures, making it a key technology for advancing the accuracy of bioprinted 3D organ models. This approach holds immense promise for biomedical applications, where

DLP-printed medical models can replicate real physiological conditions with high accuracy, which is crucial for accurately positioning scaffolds within the body and constructing tissue microstructures. The high-resolution and precision of DLP printing enable detailed tissue and organ engineering, contributing to advancements in transplantation, disease research, and drug discovery.

Technological progress in DLP-based 3D printing has been driven by advances in printing equipment and the development of new materials. For instance, continuous liquid interface production has significantly enhanced the resolution and speed of DLP 3D printing, enabling the fabrication of volumetric structures in a single, streamlined process [136,137]. In addition, the introduction of a wider range of materials, including functional materials, initiator-free systems, and non-toxic photoinitiators, has further broadened the scope of DLP-based 3D printing applications [138–140]. These innovations are paving the way for more sophisticated and biocompatible 3D printing materials, making the technology more viable for medical and clinical use.

Despite these advancements, DLP-based bioink 3D printing faces several challenges. A major limitation is the restricted material selection, which is currently limited to photosensitive polymers. This constraint excludes a vast array of biocompatible biomaterials that have been developed for medical applications. To incorporate these biomaterials into DLP printing, they must either be combined with photosensitive polymers or chemically modified with photosensitive groups, thus adding complexity to the process. In addition, many photoinitiators used to trigger polymerization are toxic, raising concerns about the biocompatibility of printed structures, particularly in clinical applications.

Another challenge inherent to the DLP printing process, particularly the vat photopolymerization method, is increased material waste compared with extrusion-based 3D printing methods. In addition, the repetitive mechanical stress caused by the lowering and lifting of the print platform during the process can compromise the mechanical integrity of the printed structures, potentially resulting in deformation or weakened materials.

To address these challenges, future advancements in DLP-based bioink printing will need to prioritize the development of versatile and biocompatible materials [141]. Promising innovations are already emerging, including functional materials, non-toxic photoinitiators, and initiator-free systems, which could help reduce the reliance on traditional photosensitive polymers. In addition, identifying new bioinks that can be directly used in DLP printing without photosensitive modifications is crucial for expanding the range of available materials.

Improving printing equipment will also be key to addressing some of these challenges. Continuous liquid interface production has already demonstrated the potential to enhance both the resolution and speed of DLP 3D printing, enabling the creation of volumetric structures in a single step [142]. Further innovations could focus on minimizing mechanical stress during the printing process by reducing or eliminating the need for repetitive lifting of the print platform. Such advances would improve print quality, reduce material deformation, and enhance the overall durability of printed structures.

From a regulatory viewpoint, extensive clinical research is required to evaluate the safety, efficacy, and long-term stability of 3D-printed medical products. This research will be instrumental in informing regulatory policies and supporting the clinical translation of DLP-based 3D printing technologies into healthcare settings. In addition, the development of comprehensive regulatory frameworks will be necessary to ensure the safe and widespread adoption of DLP-printed scaffolds and tissues in medical applications.

In future research, bioink development must prioritize not only physical and chemical stability but also structural integrity and mechanical performance in clinically relevant environments. Collaborative efforts between material scientists, engineers, and medical researchers will be vital in optimizing material formulations, printing parameters, and scaffold designs to produce functional, biocompatible structures

suitable for tissue regeneration and therapeutic applications. By overcoming these challenges, DLP-based 3D printing has the potential to revolutionize regenerative medicine, offering precise, customizable solutions for tissue engineering, organ transplantation, and personalized medicine.

Competing financial interests

The authors declare no competing financial interests.

CRediT authorship contribution statement

Yun Geun Jeong: Formal analysis, Data curation. **James J. Yoo:** Data curation, Conceptualization. **Sang Jin Lee:** Data curation, Conceptualization. **Moon Suk Kim:** Writing – review & editing, Writing – original draft, Supervision, Funding acquisition, Conceptualization.

Declaration of competing interest

The authors declare the following financial interests/personal relationships which may be considered as potential competing interests: Moon Suk Kim reports financial support was provided by Ajou University. Moon Suk Kim reports a relationship with Ajou University that includes: employment. If there are other authors, they declare that they have no known competing financial interests or personal relationships that could have appeared to influence the work reported in this paper.

Data availability

Data will be made available on request.

Acknowledgments

This study was supported by the National Research Foundation of Korea (NRF) grants, Creative Materials Discovery Program (2019M3D1A1078938) and Future Promising Fusion Technology Pioneer Program (RS-2024-00458419).

References

- [1] L. Ma, S. Yu, X. Xu, S.M. Amadi, J. Zhang, Z. Wang, Application of artificial intelligence in 3d printing physical organ models, *Mater. Today Bio* 23 (2023) 100792.
- [2] A. Opara, P. Canning, A. Alwan, E.C. Opara, Challenges and perspectives for future considerations in the bioengineering of a bioartificial pancreas, *Ann. Biomed. Eng.* 52 (7) (2024) 1795–1803.
- [3] R.P. Xian, C.L. Walsh, S.E. Verleden, W.L. Wagner, A. Bellier, S. Marussi, M. Ackermann, D.D. Jonigk, J. Jacob, P.D. Lee, P. Tafforeau, A multiscale x-ray phase-contrast tomography dataset of a whole human left lung, *Sci. Data* 9 (1) (2022) 264.
- [4] K. Buckley, J.G. Kerns, A.W. Parker, A.E. Goodship, P. Matousek, Millimeter-scale mapping of cortical bone reveals organ-scale heterogeneity, *Appl. Spectrosc.* 68 (4) (2014) 510–514.
- [5] S. Dalfino, P. Savadori, M. Piazzoni, S.T. Connelly, A.B. Gianni, M. Del Fabbro, G. M. Tartaglia, L. Moroni, Regeneration of critical-sized mandibular defects using 3d-printed composite scaffolds: a quantitative evaluation of new bone formation in vivo studies, *Adv. Healthc. Mater.* 12 (21) (2023) e2300128.
- [6] R. Su, J. Chen, X. Zhang, W. Wang, Y. Li, R. He, D. Fang, 3d-printed micro/nano-scaled mechanical metamaterials: fundamentals, technologies, progress, applications, and challenges, *Small* 19 (29) (2023) e2206391.
- [7] A. Sinha, F.Z. Simnani, D. Singh, A. Nandi, A. Choudhury, P. Patel, E. Jha, R. S. Chouhan, N.K. Kaushik, Y.K. Mishra, P.K. Panda, M. Suar, S.K. Verma, The translational paradigm of nanobiomaterials: biological chemistry to modern applications, *Mater. Today Bio* 17 (2022) 100463.
- [8] D. Lu, Y. Yang, P. Zhang, Z. Ma, W. Li, Y. Song, H. Feng, W. Yu, F. Ren, T. Li, H. Zeng, J. Wang, Development and application of three-dimensional bioprinting scaffold in the repair of spinal cord injury, *Tissue Eng. Regen. Med.* 19 (6) (2022) 1113–1127.
- [9] M. Altunbek, F. Afghah, O.S. Caliskan, J.J. Yoo, B. Koc, Design and bioprinting for tissue interfaces, *Biofabrication* 15 (2) (2023).
- [10] F. Cadamuro, F. Nicotra, L. Russo, 3d printed tissue models: from hydrogels to biomedical applications, *J. Control. Release* 354 (2023) 726–745.
- [11] J.S. Young, M. McAllister, M.B. Marshall, Three-dimensional technologies in chest wall resection and reconstruction, *J. Surg. Oncol.* 127 (2) (2023) 336–342.
- [12] S. Sadeghzade, J. Liu, H. Wang, X. Li, J. Cao, H. Cao, B. Tang, H. Yuan, Recent advances on bioactive baghdadite ceramic for bone tissue engineering applications: 20 years of research and innovation (a review), *Mater. Today Bio* 17 (2022) 100473.
- [13] Y.B. Ji, J.Y. Park, Y. Kang, S. Lee, H.J. Ju, S. Choi, B.Y. Lee, M.S. Kim, Scaffold printing using biodegradable poly(1,4-butylene carbonate) ink: printability, in vivo physicochemical properties, and biocompatibility, *Mater. Today Bio* 12 (2021) 100129.
- [14] S.H. Kim, J.S. Kwon, J.G. Cho, K.G. Park, T.H. Lim, M.S. Kim, H.S. Choi, C. H. Park, S.J. Lee, Non-invasive in vivo monitoring of transplanted stem cells in 3d-bioprinted constructs using near-infrared fluorescent imaging, *Bioeng. Transl. Med.* 6 (2) (2021) e10216.
- [15] D.Y. Kwon, J.Y. Park, B.Y. Lee, M.S. Kim, Comparison of scaffolds fabricated via 3d Printing and salt leaching: in vivo imaging, biodegradation, and inflammation, *Polymers* 12 (10) (2020).
- [16] S.H. Kim, J.H. Park, J.S. Kwon, J.G. Cho, K.G. Park, C.H. Park, J.J. Yoo, A. Atala, H.S. Choi, M.S. Kim, S.J. Lee, NIR fluorescence for monitoring in vivo scaffold degradation along with stem cell tracking in bone tissue engineering, *Biomaterials* 258 (2020) 120267.
- [17] D.Y. Kwon, J.H. Park, S.H. Jang, J.Y. Park, J.W. Jang, B.H. Min, W.D. Kim, H. B. Lee, J. Lee, M.S. Kim, Bone regeneration by means of a three-dimensional printed scaffold in a rat cranial defect, *Tissue Eng. Regen. Med.* 12 (2) (2018) 516–528.
- [18] D. Yeon Kwon, J. Seon Kwon, S. Hun Park, J. Hun Park, S. Hee Jang, X. Yun Yin, J.-H. Yun, J. Ho Kim, B. Hyun Min, J. Hee Lee, W.-D. Kim, M. Suk Kim, A computer-designed scaffold for bone regeneration within cranial defect using human dental pulp stem cells, *Sci. Rep.* 5 (1) (2015) 12721.
- [19] W. Zhu, X. Ma, M. Gou, D. Mei, K. Zhang, S. Chen, 3d printing of functional biomaterials for tissue engineering, *Curr. Opin. Biotechnol.* 40 (2016) 103–112.
- [20] M. Castilho, M. de Ruijter, S. Beirne, C.C. Villette, K. Ito, G.G. Wallace, J. Malda, Multitechnology biofabrication: a new approach for the manufacturing of functional tissue structures? *Trends Biotechnol.* 38 (12) (2020) 1316–1328.
- [21] Z.T. Xie, J. Zeng, S. Miyagawa, Y. Sawa, M. Matsusaki, 3d puzzle-inspired construction of large and complex organ structures for tissue engineering, *Mater. Today Bio* 21 (2023) 100726.
- [22] J. Yang, X. An, B. Lu, H. Cao, Z. Cheng, X. Tong, H. Liu, Y. Ni, Lignin: a multifaceted role/function in 3d printing inks, *Int. J. Biol. Macromol.* 267 (2024) 131364.
- [23] J.H. Larry, Digital light processing for high-brightness high-resolution applications, *Proc. SPIE* (1997) 27–40.
- [24] Y. Fang, Y. Guo, T. Liu, R. Xu, S. Mao, X. Mo, T. Zhang, L. Ouyang, Z. Xiong, W. Sun, Advances in 3d bioprinting, *Chin. J. Mech. Eng. Addit. Manuf. Front.* 1 (1) (2022) 100011.
- [25] C.M. Leung, P. De Haan, K. Ronaldson-Bouchard, G.-A. Kim, J. Ko, H.S. Rho, Z. Chen, P. Habibovic, N.L. Jeon, S. Takayama, A guide to the organ-on-a-chip, *Nat. Rev. Methods Primers* 2 (1) (2022) 33.
- [26] L.J. Hornbeck, W.E. Nelson, Bistable Deformable Mirror Device, *Spatial Light Modulators and Applications*, Opt. Publ. Group, 1988, p. ThB2.
- [27] A. Frederiksen, R. Fiess, W. Stork, S. Bogatscher, N. Heußner, Eye safety for scanning laser projection systems, *Biomed. Tech. Biomed. Eng.* 57 (3) (2012) 175–184.
- [28] A. Amini, R.M. Guijt, T. Themelis, J. De Vos, S. Eeltink, Recent developments in digital light processing 3d-printing techniques for microfluidic analytical devices, *J. Chromatogr. A* 1692 (2023) 463842.
- [29] H.K. Balakrishnan, E.H. Doeven, A. Merenda, L.F. Dumée, R.M. Guijt, 3d printing for the integration of porous materials into miniaturised fluidic devices: a review, *Anal. Chim. Acta* 1185 (2021) 338796.
- [30] J.L. Sanchez Noriega, N.A. Chartrand, J.C. Valdoz, C.G. Cribbs, D.A. Jacobs, D. Poulson, M.S. Viglione, A.T. Woolley, P.M. Van Ry, K.A. Christensen, Spatially and optically tailored 3d printing for highly miniaturized and integrated microfluidics, *Nat. Commun.* 12 (1) (2021) 5509.
- [31] Y. Gao, D. Zhou, J. Lyu, Q. Xu, B. Newland, K. Matyjaszewski, H. Tai, W. Wang, Complex polymer architectures through free-radical polymerization of multivinyl monomers, *Nat. Rev. Chem* 4 (4) (2020) 194–212.
- [32] X. Lopez de Pariza, O. Varela, S.O. Catt, T.E. Long, E. Blasco, H. Sardon, Recyclable photoresins for light-mediated additive manufacturing towards loop 3d printing, *Nat. Commun.* 14 (1) (2023) 5504.
- [33] J.H. Jorge, E.T. Giampaolo, A.L. Machado, C.E. Vergani, Cytotoxicity of denture base acrylic resins: a literature review, *J. Prosthet. Dent* 90 (2) (2003) 190–193.
- [34] L. de Silva, P.N. Bernal, A. Rosenberg, J. Malda, R. Levato, D. Gawlitta, Biofabricating the vascular tree in engineered bone tissue, *Acta Biomater.* 156 (2023) 250–268.
- [35] D.J. Munoz-Pinto, A.C. Jimenez-Vergara, T.P. Gharat, M.S. Hahn, Characterization of sequential collagen-poly(ethylene glycol) diacrylate interpenetrating networks and initial assessment of their potential for vascular tissue engineering, *Biomaterials* 40 (2015) 32–42.
- [36] L. Hu, T. Li, X. Wu, L. Yu, G. Zeng, M. Han, J. Xu, Z. Wang, L. Wang, D. Xu, Stretchable alginate/GelMA interpenetrating network (IPN) hydrogel microspheres based on coaxial microfluidic technique for skeletal muscle tissue engineering, *Colloids Surf. A: Physicochem. Eng. Asp.* 687 (2024) 133502.
- [37] S. Pal, S.K. Asha, Thiol-ene-based degradable 3d printed network from bio resource derived monomers ethyl-lactate and isosorbide, *Eur. Polym. J.* 205 (2024) 112761.
- [38] N.K. Mandsberg, F. Aslan, Z. Dong, P.A. Levkin, 3d printing of reactive macroporous polymers via thiol-ene chemistry and polymerization-induced phase separation, *Chem. Comm.* 60 (45) (2024) 5872–5875.

- [39] A. GhavamiNejad, N. Ashammakhi, X.Y. Wu, A. Khademhosseini, Crosslinking strategies for 3d bioprinting of polymeric hydrogels, *Small* 16 (35) (2020) e2002931.
- [40] H. Jiang, X. Li, T. Chen, Y. Liu, Q. Wang, Z. Wang, J. Jia, Bioprinted vascular tissue: assessing functions from cellular, tissue to organ levels, *Mater. Today Bio* 23 (2023) 100846.
- [41] A. Bhattacharyya, M.R. Khatun, S. Narmatha, R. Nagarajan, I. Noh, Modulation of 3d bioprintability in polysaccharide bioink by bioglass nanoparticles and multiple metal ions for tissue engineering, *Tissue Eng. Regen. Med.* 21 (2) (2024) 261–275.
- [42] Q. Wang, Y. Zhang, Y. Ma, M. Wang, G. Pan, Nano-crosslinked dynamic hydrogels for biomedical applications, *Mater. Today Bio* 20 (2023) 100640.
- [43] K. Mokhtarinia, E. Maseali, Post-decellularized printing of cartilage extracellular matrix: distinction between biomaterial ink and bioink, *Biomater. Sci.* 11 (7) (2023) 2317–2329.
- [44] X. Mao, Z. Wang, Research progress of three-dimensional bioprinting artificial cardiac tissue, *Tissue Eng. Regen. Med.* 20 (1) (2023) 1–9.
- [45] M. Keshavarz, M. Jahanshahi, M. Hasany, F.B. Kadumudi, M. Mehrali, M. A. Shahbazi, P. Alizadeh, G. Orive, A. Dolatshahi-Pirouz, Smart alginate inks for tissue engineering applications, *Mater. Today Bio* 23 (2023) 100829.
- [46] M. Kasturi, V. Mathur, M. Gadre, V. Srinivasan, K.S. Vasanthan, Three dimensional bioprinting for hepatic tissue engineering: from in vitro models to clinical applications, *Tissue Eng. Regen. Med.* 21 (1) (2023) 21–52.
- [47] A. Guo, S. Zhang, R. Yang, C. Sui, Enhancing the mechanical strength of 3d printed GelMA for soft tissue engineering applications, *Mater. Today Bio* 24 (2024) 100939.
- [48] S. Asim, T.A. Tabish, U. Liaqat, I.T. Ozbolat, M. Rizwan, Advances in gelatin bioinks to optimize bioprinted cell functions, *Adv. Healthc. Mater.* 12 (17) (2023) e2203148.
- [49] H. Wang, H. Yu, X. Zhou, J. Zhang, H. Zhou, H. Hao, L. Ding, H. Li, Y. Gu, J. Ma, J. Qiu, D. Ma, An overview of extracellular matrix-based bioinks for 3d bioprinting, *Front. Bioeng. Biotechnol.* 10 (2022) 905438.
- [50] L. Elomaa, A. Almalla, E. Keshi, K.H. Hillebrandt, I.M. Sauer, M. Weinhart, Rise of tissue- and species-specific 3d bioprinting based on decellularized extracellular matrix-derived bioinks and bioresins, *Biomaterials and Biosystems* 12 (2023) 100084.
- [51] C. Li, Z. Zheng, J. Jia, W. Zhang, L. Qin, W. Zhang, Y. Lai, Preparation and characterization of photocurable composite extracellular matrix-methacrylated hyaluronic acid bioink, *J. Mater. Chem. B* 10 (22) (2022) 4242–4253.
- [52] S.O. Sarrigiannidis, J.M. Rey, O. Dobre, C. González-García, M.J. Dalby, M. Salmeron-Sanchez, A tough act to follow: collagen hydrogel modifications to improve mechanical and growth factor loading capabilities, *Mater. Today Bio* 10 (2021) 100098.
- [53] B. Zhou, X. Jiang, X. Zhou, W. Tan, H. Luo, S. Lei, Y. Yang, GelMA-based bioactive hydrogel scaffolds with multiple bone defect repair functions: therapeutic strategies and recent advances, *Biomater. Res.* 27 (1) (2023) 86.
- [54] J.J.Y. Tan, C.P. Lee, M. Hashimoto, Preheating of gelatin improves its printability with transglutaminase in direct ink writing 3d printing, *Int. J. Bioprinting* 6 (4) (2020) 296.
- [55] Y. Zhang, H. Chen, J. Li, Recent advances on gelatin methacrylate hydrogels with controlled microstructures for tissue engineering, *Int. J. Biol. Macromol.* 221 (2022) 91–107.
- [56] K. Choi, C.Y. Park, J.S. Choi, Y.J. Kim, S. Chung, S. Lee, C.H. Kim, S.J. Park, The effect of the mechanical properties of the 3d printed gelatin/hyaluronic acid scaffolds on hMSCs differentiation towards chondrogenesis, *Tissue Eng. Regen. Med.* 20 (4) (2023) 593–605.
- [57] J. Zong, Q. He, Y. Liu, M. Qiu, J. Wu, B. Hu, Advances in the development of biodegradable coronary stents: a translational perspective, *Mater. Today Bio* 16 (2022) 100368.
- [58] S. Swetha, K. Lavanya, R. Sruthi, N. Selvamurugan, An insight into cell-laden 3d-printed constructs for bone tissue engineering, *J. Mater. Chem. B* 8 (43) (2020) 9836–9862.
- [59] D. Petta, U. D'Amora, L. Ambrosio, D.W. Grijpma, D. Eglin, M. D'Este, Hyaluronic acid as a bioink for extrusion-based 3d printing, *Biofabrication* 12 (3) (2020) 032001.
- [60] P. Prabhakaran, T. Palaniyandi, B. Kanagavalli, V. Ram Kumar, R. Hari, V. Sandhiya, G. Baskar, B.K. Rajendran, A. Sivaji, Prospect and retrospect of 3d bio-printing, *Acta Histochem.* 124 (7) (2022) 151932.
- [61] S.C. Gauci, A. Vranic, E. Blasco, S. Brase, M. Wegener, C. Barner-Kowollik, Photochemically activated 3d printing inks: current status, challenges, and opportunities, *Adv. Mater.* 36 (3) (2024) e2306468.
- [62] A. Bandyopadhyay, B.B. Mandal, N. Bhardwaj, 3d bioprinting of photo-crosslinkable silk methacrylate (SiMA)-polyethylene glycol diacrylate (PEGDA) bioink for cartilage tissue engineering, *J. Biomed. Mater. Res.* 110 (4) (2022) 884–898.
- [63] M. Hakim Khalili, R. Zhang, S. Wilson, S. Goel, S.A. Impey, A.I. Aria, Additive manufacturing and physicomechanical characteristics of PEGDA hydrogels: recent advances and perspective for tissue engineering, *Polymers* 15 (10) (2023).
- [64] C. Zhong, H. Xu, Advances in the construction of in vitro liver tissue models using 3d bioprinting technology, *Hepatobiliary Surg. Nutr.* 12 (5) (2023) 806.
- [65] J. Wang, Y. Shi, B. Mao, B. Zhang, J. Yang, Z. Hu, W. Liao, Biomaterials for inflammatory bowel disease: treatment, diagnosis and organoids, *Appl. Mater. Today* 36 (2024) 102078.
- [66] M. Hakim Khalili, Physicochemical and Nanomechanical Behaviour of 3d Printed PEGDA Hydrogel Structures for Tissue Engineering Applications, Cranfield University, 2023.
- [67] J.S. Kim, S. Hong, C. Hwang, Bio-ink materials for 3d bio-printing, *J. Int. Spc. Simul. Surg.* 3 (2) (2016) 49–59.
- [68] S.M. Bittner, H.A. Pearce, K.J. Hogan, M.M. Smoak, J.L. Guo, A.J. Melchiorri, D. W. Scott, A.G. Mikos, Swelling behaviors of 3d printed hydrogel and hydrogel-microcarrier composite scaffolds, *Tissue Eng. Part A* 27 (11–12) (2021) 665–678.
- [69] Y. Wang, B.J. Sheppard, R. Langer, Poly(glycerol sebacate) - a novel biodegradable elastomer for tissue engineering, *Mat. Res. Soc. Symp. Proc.* 724 (2002) 223.
- [70] E. Hamed, N. Vahedi, F. Sigaroodi, A. Parandakh, S. Hosseinzadeh, F. Zeinali, M. M. Khani, Recent progress of bio-printed PEGDA-based bioinks for tissue regeneration, *Polym. Adv. Technol.* 34 (11) (2023) 3505–3517.
- [71] G. Lu, R. Tang, J. Nie, X. Zhu, Photocuring 3d printing of hydrogels: techniques, materials, and applications in tissue engineering and flexible devices, *Macromol. Rapid Commun.* 45 (7) (2024) e2300661.
- [72] Z. Wu, C. Boyer, Near-infrared light-induced reversible deactivation radical polymerization: expanding frontiers in photopolymerization, *Adv. Sci.* 10 (33) (2023) e2304942.
- [73] Q. Zhang, H.P. Bei, M. Zhao, Z. Dong, X. Zhao, Shedding light on 3d printing: printing photo-crosslinkable constructs for tissue engineering, *Biomaterials* 286 (2022) 121566.
- [74] K.S. Lim, J.H. Galarraga, X. Cui, G.C.J. Lindberg, J.A. Burdick, T.B.F. Woodfield, Fundamentals and applications of photo-cross-linking in bioprinting, *Chem. Rev.* 120 (19) (2020) 10662–10694.
- [75] S. You, P. Wang, J. Schimelman, H.H. Hwang, S. Chen, High-fidelity 3d printing using flashing photopolymerization, *Addit. Manuf.* 30 (2019).
- [76] J. Liu, K. Miller, X. Ma, S. Dewan, N. Lawrence, G. Whang, P. Chung, A. D. McCulloch, S. Chen, Direct 3d bioprinting of cardiac micro-tissues mimicking native myocardium, *Biomaterials* 256 (2020) 120204.
- [77] D. Xue, Y. Wang, J. Zhang, D. Mei, Y. Wang, S. Chen, Projection-based 3d printing of cell patterning scaffolds with multiscale channels, *ACS Appl. Mater. Interfaces* 10 (23) (2018) 19428–19435.
- [78] A.K. Miri, D. Nieto, L. Iglesias, H. Goodarzi Hosseinabadi, S. Maharjan, G.U. Ruiz-Esparza, P. Khoshakhlagh, A. Manbachi, M.R. Dokmeci, S. Chen, S.R. Shin, Y. S. Zhang, A. Khademhosseini, Microfluidics-enabled multimaterial maskless stereolithographic bioprinting, *Adv. Mater.* 30 (27) (2018) e1800242.
- [79] W. Zhu, X. Qu, J. Zhu, X. Ma, S. Patel, J. Liu, P. Wang, C.S. Lai, M. Gou, Y. Xu, K. Zhang, S. Chen, Direct 3d bioprinting of prevascularized tissue constructs with complex microarchitecture, *Biomaterials* 124 (2017) 106–115.
- [80] X. Ma, X. Qu, W. Zhu, Y.S. Li, S. Yuan, H. Zhang, J. Liu, P. Wang, C.S. Lai, F. Zanella, G.S. Feng, F. Sheikh, S. Chien, S. Chen, Deterministically patterned biomimetic human iPSC-derived hepatic model via rapid 3d bioprinting, *Proc. Natl. Acad. Sci. U.S.A.* 113 (8) (2016) 2206–2211.
- [81] Z. Zhong, X. Deng, P. Wang, C. Yu, W. Kiratitanaporn, X. Wu, J. Schimelman, M. Tang, A. Balayan, E. Yao, J. Tian, L. Chen, K. Zhang, S. Chen, Rapid bioprinting of conjunctival stem cell micro-constructs for subconjunctival ocular injection, *Biomaterials* 267 (2021) 120462.
- [82] P. Wang, X. Li, W. Zhu, Z. Zhong, A. Moran, W. Wang, K. Zhang, C. Shaochen, 3d bioprinting of hydrogels for retina cell culturing, *Bioprinting* 11 (2018).
- [83] A. Bhusal, E. Dogan, H.A. Nguyen, O. Labutina, D. Nieto, A. Khademhosseini, A. K. Miri, Multi-material digital light processing bioprinting of hydrogel-based microfluidic chips, *Biofabrication* 14 (1) (2021).
- [84] T. Lam, T. Dehne, J.P. Kruger, S. Hondke, M. Endres, A. Thomas, R. Lauster, M. Sittinger, L. Kloke, Photopolymerizable gelatin and hyaluronic acid for stereolithographic 3D bioprinting of tissue-engineered cartilage, *J. Biomed. Mater. Res. B Appl. Biomater.* 107 (8) (2019) 2649–2657.
- [85] A. Thomas, I. Orellano, T. Lam, B. Noichl, M.A. Geiger, A.K. Amler, A.E. Kreuder, C. Palmer, G. Duda, R. Lauster, L. Kloke, Vascular bioprinting with enzymatically degradable bioinks via multi-material projection-based stereolithography, *Acta Biomater.* 117 (2020) 121–132.
- [86] W. Zhu, K.R. Tringale, S.A. Woller, S. You, S. Johnson, H. Shen, J. Schimelman, M. Whitney, J. Steinauer, W. Xu, T.L. Yaksh, Q.T. Nguyen, S. Chen, Rapid continuous 3d printing of customizable peripheral nerve guidance conduits, *Mater. Today* 21 (9) (2018) 951–959.
- [87] B. Grigoryan, S.J. Paulsen, D.C. Corbett, D.W. Sazer, C.L. Fortin, A.J. Zaita, P. T. Greenfield, N.J. Calafat, J.P. Gounley, A.H. Ta, F. Johansson, A. Randles, J. E. Rosenkrantz, J.D. Louis-Rosenberg, P.A. Galie, K.R. Stevens, J.S. Miller, Multivascular networks and functional intravascular topologies within biocompatible hydrogels, *Science* 364 (6439) (2019) 458–464.
- [88] Y. Shen, H. Tang, X. Huang, R. Hang, X. Zhang, Y. Wang, X. Yao, DLP printing photocurable chitosan to build bio-constructs for tissue engineering, *Carbohydr. Polym.* 235 (2020) 115970.
- [89] G. Melilli, I. Carmagnola, C. Tonda-Turo, F. Pirri, G. Ciardelli, M. Sangermano, M. Hakkarainen, A. Chiappone, DLP 3d printing meets lignocellulosic biopolymers: carboxymethyl cellulose inks for 3d biocompatible hydrogels, *Polymers* 12 (8) (2020).
- [90] S.H. Kim, Y.K. Yeon, J.M. Lee, J.R. Chao, Y.J. Lee, Y.B. Seo, M.T. Sultan, O.J. Lee, J.S. Lee, S.I. Yoon, I.S. Hong, G. Khang, S.J. Lee, J.J. Yoo, C.H. Park, Precisely printable and biocompatible silk fibroin bioink for digital light processing 3d printing, *Nat. Commun.* 9 (1) (2018) 1620.
- [91] Z. Wang, R. Abdulla, B. Parker, R. Samanipour, S. Ghosh, K. Kim, A simple and high-resolution stereolithography-based 3d bioprinting system using visible light crosslinkable bioinks, *Biofabrication* 7 (4) (2015) 045009.
- [92] Z. Wang, Development of a Visible Light Stereolithography-Based Bioprinting System for Tissue Engineering, 2016. TJU.

- [93] X. Kuang, J. Wu, K. Chen, Z. Zhao, Z. Ding, F. Hu, D. Fang, H.J. Qi, Grayscale digital light processing 3d printing for highly functionally graded materials, *Sci. Adv.* 5 (5) (2019) e5790.
- [94] A. Bagheri, J. Jin, Photopolymerization in 3d printing, *ACS Appl. Polym. Mater.* 1 (4) (2019) 593–611.
- [95] K.S. Lim, R. Levato, P.F. Costa, M.D. Castilho, C.R. Alcalá-Orozco, K.M.A. van Dorenmalen, F.P.W. Melchels, D. Gawlitta, G.J. Hooper, J. Malda, T.B. F. Woodfield, Bio-resin for high resolution lithography-based biofabrication of complex cell-laden constructs, *Biofabrication* 10 (3) (2018) 034101.
- [96] W. Li, M. Wang, L.S. Mille, J.A. Robledo Lara, V. Huerta, T. Uribe Velazquez, F. Cheng, H. Li, J. Gong, T. Ching, C.A. Murphy, A. Llesha, S. Hassan, T.B. F. Woodfield, K.S. Lim, Y.S. Zhang, A smartphone-enabled portable digital light processing 3d printer, *Adv. Mater.* 33 (35) (2021) e2102153.
- [97] Y. Chen, J. Zhang, X. Liu, S. Wang, J. Tao, Y. Huang, W. Wu, Y. Li, K. Zhou, X. Wei, S. Chen, X. Li, X. Xu, L. Cardon, Z. Qian, M. Gou, Noninvasive in vivo 3d bioprinting, *Sci. Adv.* 6 (23) (2020) e7406.
- [98] M. Regehy, Y. Garmshausen, M. Reuter, N.F. Konig, E. Israel, D.P. Kelly, C. Y. Chou, K. Koch, B. Asfari, S. Hecht, Xolography for linear volumetric 3d printing, *Nature* 588 (7839) (2020) 620–624.
- [99] H. Kwak, S. Shin, H. Lee, J. Hyun, Formation of a keratin layer with silk fibroin-polyethylene glycol composite hydrogel fabricated by digital light processing 3d printing, *J. Ind. Eng. Chem.* 72 (2019) 232–240.
- [100] H.B. Musgrove, M.A. Catterton, R.R. Pompano, Applied tutorial for the design and fabrication of biomicrofluidic devices by resin 3dprinting, *Anal. Chim. Acta* 1209 (2022) 339842.
- [101] X. Mo, L. Ouyang, Z. Xiong, T. Zhang, Advances in digital light processing of hydrogels, *Biomed. Mater.* 17 (4) (2022) 042002.
- [102] H. Goodarzi Hosseinabadi, E. Dogan, A.K. Miri, L. Ionov, Digital light processing bioprinting advances for microtissue models, *ACS Biomater. Sci. Eng.* 8 (4) (2022) 1381–1395.
- [103] S. You, Y. Xiang, H.H. Hwang, D.B. Berry, W. Kiratitanaporn, J. Guan, E. Yao, M. Tang, Z. Zhong, X. Ma, High cell density and high-resolution 3d bioprinting for fabricating vascularized tissues, *Sci. Adv.* 9 (8) (2023) eade7923.
- [104] A. Bhusal, E. Dogan, H.A. Nguyen, O. Labutina, D. Nieto, A. Khademhosseini, A. K. Miri, Multi-material digital light processing bioprinting of hydrogel-based microfluidic chips, *Biofabrication* 14 (1) (2021) 014103.
- [105] W. Sun, Y. Chiang, C. Tsuei, Optical design for the DLP pocket projector using LED light source, *Phys. Procedia* 19 (2011) 301–307.
- [106] J. Gong, Y. Qian, K. Lu, Z. Zhu, L. Siow, C. Zhang, S. Zhou, T. Gu, J. Yin, M. Yu, H. Wang, H. Yang, Digital light processing (DLP) in tissue engineering: from promise to reality, and perspectives, *Biomed. Mater.* 17 (6) (2022) 062004.
- [107] S.H. Kim, D.Y. Kim, T.H. Lim, C.H. Park, Silk fibroin bioinks for digital light processing (DLP) 3d bioprinting, *Adv. Exp. Med. Biol.* 1249 (2020) 53–66.
- [108] M.J. Mannel, E. Baysak, J. Thiele, Fabrication of microfluidic devices for emulsion formation by microstereolithography, *Molecules* 26 (9) (2021) 2817.
- [109] U. Shashikumar, A. Saraswat, K. Deshmukh, C.M. Hussain, P. Chandra, P.C. Tsai, P.C. Huang, Y.H. Chen, L.Y. Ke, Y.C. Lin, S. Chawla, V.K. Ponnusamy, Innovative technologies for the fabrication of 3D/4D smart hydrogels and its biomedical applications - a comprehensive review, *Adv. Colloid Interface Sci.* 328 (2024) 103163.
- [110] Q. Mao, Y. Wang, Y. Li, S. Juengpanich, W. Li, M. Chen, J. Yin, J. Fu, X. Cai, Fabrication of liver microtissue with liver decellularized extracellular matrix (dECM) bioink by digital light processing (DLP) bioprinting, *Mater. Sci. Eng. C* 109 (2020) 110625.
- [111] T.Y. Lu, Y. Xiang, M. Tang, S. Chen, 3D printing approaches to engineer cardiac tissue, *Curr. Cardiol. Rep.* 25 (2023) 505–514.
- [112] Y. Wang, H. Cui, Y. Wang, C. Xu, T.J. Esworthy, S.Y. Hann, M. Boehm, Y.L. Shen, D. Mei, L.G. Zhang, 4d printed cardiac construct with aligned myofibers and adjustable curvature for myocardial regeneration, *ACS Appl. Mater. Interfaces* 13 (11) (2021) 12746–12758.
- [113] Y. Shanjani, C.C. Pan, L. Elomaa, Y. Yang, A novel bioprinting method and system for forming hybrid tissue engineering constructs, *Biofabrication* 7 (4) (2015) 045008.
- [114] L. Silva, P.N. Bernal, A.J.W. Rosenberg, J. Malda, R. Levato, D. Gawlitta, Biofabricating the vascular tree in engineered bone tissue, *Acta Biomater.* 156 (2023) 250–268.
- [115] A.K. Miri, D. Nieto, L. Iglesias, H. Goodarzi Hosseinabadi, S. Maharjan, G.U. Ruiz-Esparza, P. Khoshakhlagh, A. Manbachi, M.R. Dokmeci, S. Chen, S.R. Shin, Y. S. Zhang, A. Khademhosseini, Microfluidics-enabled multimaterial maskless stereolithographic bioprinting, *Adv. Mater.* 30 (27) (2018) e1800242.
- [116] W. Li, M. Wang, H. Ma, F.A. Chapa-Villarreal, A.O. Lobo, Y.S. Zhang, Stereolithography apparatus and digital light processing-based 3d bioprinting for tissue fabrication, *iScience* 26 (2023) 106039.
- [117] X. Xie, S. Wu, S. Mou, N. Guo, Z. Wang, J. Sun, Microtissue-based bioink as a chondrocyte microshelter for DLP bioprinting, *Adv. Healthc. Mater.* 11 (22) (2022) e2201877.
- [118] H. Hong, Y.B. Seo, D.Y. Kim, J.S. Lee, Y.J. Lee, H. Lee, O. Ajiteru, M.T. Sultan, O. J. Lee, S.H. Kim, C.H. Park, Digital light processing 3d printed silk fibroin hydrogel for cartilage tissue engineering, *Biomaterials* 232 (2020) 119679.
- [119] Z. Zhong, J. Wang, J. Tian, X. Deng, A. Balayan, Y. Sun, Y. Xiang, J. Guan, J. Schimelman, H. Hwang, S. You, X. Wu, C. Ma, X. Shi, E. Yao, S.X. Deng, S. Chen, Rapid 3d bioprinting of a multicellular model recapitulating pterygium microenvironment, *Biomaterials* 282 (2022) 121391.
- [120] M. Tang, Q. Xie, R.C. Gimple, Z. Zhong, T. Tam, J. Tian, R.L. Kidwell, Q. Wu, B. C. Prager, Z. Qiu, A. Yu, Z. Zhu, P. Mesci, H. Jing, Y. Schimelman, P. Wang, D. Lee, M.H. Lorenzini, D. Dixit, L. Zhao, S. Bhargava, T.E. Miller, X. Wan, J. Tang, B. Sun, B.F. Cravatt, A.R. Muotri, S. Chen, J.N. Rich, Three-dimensional bioprinted glioblastoma microenvironments model cellular dependencies and immune interactions, *Cell Res.* 30 (10) (2020) 833–853.
- [121] C. Yu, X. Ma, W. Zhu, P. Wang, K.L. Miller, J. Stupin, A. Koroleva-Maharajh, A. Hairabedian, S. Chen, Scanningless and continuous 3d bioprinting of human tissues with decellularized extracellular matrix, *Biomaterials* 194 (2019) 1–13.
- [122] J. Zhang, D. Huang, S. Liu, X. Dong, Y. Li, H. Zhang, Z. Yang, Q. Su, W. Huang, W. Zheng, W. Zhou, Zirconia toughened hydroxyapatite biocomposite formed by a DLP 3d printing process for potential bone tissue engineering, *Mater. Sci. Eng. C* 105 (2019) 110054.
- [123] Y. Li, J. Li, S. Jiang, C. Zhong, C. Zhao, Y. Jiao, J. Shen, H. Chen, M. Ye, J. Zhou, X. Yang, Z. Gou, S. Xu, M. Shen, The design of strut/TPMS-based pore geometries in bioceramic scaffolds guiding osteogenesis and angiogenesis in bone regeneration, *Mater. Today Bio* 20 (2023) 100667.
- [124] W. Jiang, Y. Zhan, Y. Zhang, D. Sun, G. Zhang, Z. Wang, L. Chen, J. Sun, Synergistic large segmental bone repair by 3d printed bionic scaffolds and engineered ADSC nanovesicles: towards an optimized regenerative microenvironment, *Biomaterials* 308 (2024) 122566.
- [125] T.K. Liu, Y. Pang, Z.Z. Zhou, R. Yao, W. Sun, An integrated cell printing system for the construction of heterogeneous tissue models, *Acta Biomater.* 95 (2019) 245–257.
- [126] W. Kim, G. Kim, Engineered 3d liver-tissue model with minispheroids formed by a bioprinting process supported with in situ electrical stimulation, *Bioact. Mater.* 35 (2024) 382–400.
- [127] Z. Yang, L. Xie, B. Zhang, G. Zhang, F. Huo, C. Zhou, X. Liang, Y. Fan, W. Tian, Y. Tan, Preparation of BMP-2/PDA-BCP bioceramic scaffold by DLP 3d printing and its ability for inducing continuous bone formation, *Front. Bioeng. Biotechnol.* 10 (2022) 854693.
- [128] K.N. Eckstein, J.E. Hergert, A.C. Uzcategui, S.A. Schoonraad, S.J. Bryant, R. R. McLeod, V.L. Ferguson, Controlled mechanical property gradients within a digital light processing printed hydrogel-composite osteochondral scaffold, *Ann. Biomed. Eng.* 52 (8) (2024) 2162–2177.
- [129] M. Rajput, P. Mondal, P. Yadav, K. Chatterjee, Light-based 3d bioprinting of bone tissue scaffolds with tunable mechanical properties and architecture from photocurable silk fibroin, *Int. J. Biol. Macromol.* 202 (2022) 644–656.
- [130] M. Goldvaser, E. Epstein, O. Rosen, A. Jayson, N. Natan, T. Ben-Shalom, S. Saphier, S. Katalan, O. Shoseyov, Poly(vinyl alcohol)-methacrylate with CRGD peptide: a photocurable biocompatible hydrogel, *J. Tissue Eng. Regen. Med.* 16 (2) (2022) 140–150.
- [131] G. Jiang, S. Li, K. Yu, B. He, J. Hong, T. Xu, J. Meng, C. Ye, Y. Chen, Z. Shi, G. Feng, W. Chen, S. Yan, Y. He, R. Yan, A 3d-printed PRP-GelMA hydrogel promotes osteochondral regeneration through M2 macrophage polarization in a rabbit model, *Acta Biomater.* 128 (2021) 150–162.
- [132] T.Y. Yuan, J. Zhang, T. Yu, J.P. Wu, Q.Y. Liu, 3d bioprinting for spinal cord injury repair, *Front. Bioeng. Biotechnol.* 10 (2022) 847344.
- [133] A. Mora-Boza, A. Mulero-Russe, N.D. Caprio, J.A. Burdick, A. Singh, A.J. Garcia, Facile photopatterning of perfusable microchannels in synthetic hydrogels to recreate microphysiological environments, *Adv. Mater.* 35 (52) (2023) e2306765.
- [134] V. Karamzadeh, M.L. Shen, H. Shafiq, F. Lussier, D. Juncker, Nanoporous, gas permeable PEGDA ink for 3d printing organ-on-a-chip devices, *Adv. Funct. Mater.* 34 (28) (2024) 2315035.
- [135] R. Paul, Y. Zhao, D. Coster, X. Qin, K. Islam, Y. Wu, Y. Liu, Rapid prototyping of high-resolution large format microfluidic device through maskless image guided in-situ photopolymerization, *Nat. Commun.* 14 (1) (2023) 4520.
- [136] K. Hsiao, B.J. Lee, T. Samuelsen, G. Lipkowitz, J.M. Kronenfeld, D. Ilyn, A. Shih, M.T. Dulay, L. Tate, E.S.G. Shaqfeh, J.M. DeSimone, Single-digit-micrometer-resolution continuous liquid interface production, *Sci. Adv.* 8 (46) (2022) eabq2846.
- [137] J.R. Tumbleston, D. Shirvanyants, N. Ermoshkin, R. Januszewicz, A.R. Johnson, D. Kelly, K. Chen, R. Pinschmidt, J.P. Rolland, A. Ermoshkin, Continuous liquid interface production of 3d objects, *Science* 347 (6228) (2015) 1349–1352.
- [138] A.A. Pawar, G. Saada, I. Cooperstein, L. Larush, J.A. Jackman, S.R. Tabaei, N. J. Cho, S. Magdassi, High-performance 3d printing of hydrogels by water-dispersible photoinitiator nanoparticles, *Sci. Adv.* 2 (4) (2016) e1501381.
- [139] C. Yu, J. Schimelman, P. Wang, K.L. Miller, X. Ma, S. You, J. Guan, B. Sun, W. Zhu, S. Chen, Photopolymerizable biomaterials and light-based 3d printing strategies for biomedical applications, *Chem. Rev.* 120 (19) (2020) 10695–10743.
- [140] Y. Bao, Recent trends in advanced photoinitiators for vat photopolymerization 3d printing, *Macromol. Rapid Commun.* 43 (14) (2022) e2200202.
- [141] Z. Zhong, D. Eglin, M. Alini, G.R. Richards, L. Qin, Y. Lai, Visible light-induced 3d bioprinting technologies and corresponding bioink materials for tissue engineering: a review, *Engineering* 7 (7) (2021) 966–978.
- [142] B.J. Lee, K. Hsiao, G. Lipkowitz, T. Samuelsen, L. Tate, J.M. DeSimone, Characterization of a 30 μm pixel size CLIP-based 3d printer and its enhancement through dynamic printing optimization, *Addit. Manuf.* 55 (2022) 102800.